

Electrosynthesis and characterization of a new semi-conducting oligomer deriving from a disubstituted chalcone: 4-dimethylamino-4'-methoxychalcone

Ilhem Messaoudi^a, Imen Aribi^a, Zouhour Zaaboub^b, Sahbi Ayachi^c, Mohamed Othman^d, Ayoub Haj Said^{a,e,*}

^a Université de Monastir, Laboratoire Interfaces et Matériaux Avancé (LIMA), Faculté des Sciences de Monastir, Boulevard de l'environnement, 5000 Monastir, Tunisia

^b Université de Monastir, Laboratoire de Micro-opto-électronique et Nanostructures (LMON), Faculté des Sciences de Monastir, Boulevard de l'environnement, 5000 Monastir, Tunisia

^c Université de Monastir, Laboratoire de Physico-chimie des matériaux (LR01ES19), Faculté des Sciences de Monastir, Boulevard de l'environnement, 5000 Monastir, Tunisia

^d Normandie Université France, UNILEHAVRE, URCOM, EA 3221, FR 3038 CNRS, F-76600 Le Havre, France

^e Centre de Recherche en Microélectronique et Nanotechnologie, Technopôle de Sousse, BP 334, Sahloul, 4054 Sousse, Tunisia

ARTICLE INFO

Article history:

Received 28 September 2020

Revised 12 December 2020

Accepted 21 December 2020

Available online 24 December 2020

Keywords:

Chalcone

Voltammetry

Electrosynthesis

Semi-conducting oligomer

Photoluminescence

ABSTRACT

An oligo phenylene vinylene was electrosynthesized by the anodic oxidation of the 4-dimethylamino-4'-methoxychalcone (DMAMC) at a constant potential in nitromethane on a platinum electrode. ¹H and ¹³C NMR, FTIR and UV spectroscopy, confirmed the chemical structure of the obtained oligomer. In addition, the latter was thermally stable up to 190 °C and exhibited two emission peaks in the yellow-orange zone. The values of the corresponding optical and electrochemical band gaps were found to be 2.04 and 1.68 eV, respectively. Finally, a mechanism for the electro-oligomerization of DMAMC was proposed based on the experimental study and a theoretical modelisation using DFT calculation.

© 2020 Elsevier B.V. All rights reserved.

1. Introduction

Chalcone derivatives have recently attracted significant attention as part of the research of new functional materials for optoelectronics [1–4], non-linear optics [5–11], electrochemical and optical chemosensing [12–18] thanks to their ease of synthesis and the accessibility of their starting materials, their simple structural modification, and their interesting optical property.

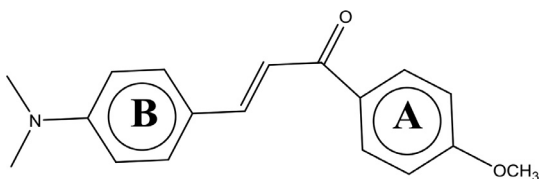
Although the electrochemical reduction of chalcones has been well-studied [19–22], few studies have been devoted to their anodic oxidation [23–26]. Particularly, flavones and flavanols have been described as the resulting compounds of the anodic oxidation of 2'-hydroxychalcones [23–25]. More recently, we were interested in the anodic oxidation of chalcones, substituted on ring B, in acetonitrile on a platinum electrode, namely the 4-methoxylated (MC)

and the 3,4,5-trimethoxylated (TMC) chalcones [1–3]. We demonstrated that, under these conditions, the electrochemical oxidation led to the formation of phenylenevinylene oligomers. In addition, we showed that the presence of the methoxy group(s) on the B ring of chalcones (scheme 1) has a crucial role in decreasing the oxidation potential and in directing the reaction scheme by conferring a distonic character to the radical cations. Indeed, the rate-limiting step in the oligomerization process was the coupling of two distonic isomers of radical cations obtained from the first anodic electron removal [1,2].

In the present work, we are interested in the anodic oxidation of a disubstituted chalcone, bearing the dimethylaminophenyl moiety. The aim of this study is to assess the influence of introducing the N,N dimethyl amino group donor on the electrochemical behavior of the chalcone at the voltammetric and preparative electrolysis timescales. In fact, N-alkyl/aryl amine, acting as a donor moiety, will affect the frontier molecular orbital energies and consequently the electrochemical and the photophysical properties. [27–32].

* Corresponding author.

E-mail addresses: ayoub.hajsaid@fsm.rnu.tn, ahajsaid@gmail.com (A.H. Said).



Scheme 1. The chemical structure of the studied chalcone (DMAMC).

The investigation of the electrochemical behavior of the 4-dimethylamino-4'-methoxychalcone (DMAMC) was carried out in nitromethane, on a platinum electrode. The choice of nitromethane was to avoid the nucleophilic attack of the solvent on the radical cations formed during the electrolysis. The obtained electrolysis material was characterized by different physico-chemical methods and its optical properties were explored. Finally, a Density functional theory (DFT) study was performed on the geometrical structure and the electron density distribution of the DMAMC radical cation. The theoretical data have been correlated to the experimental results and were exploited to propose a mechanistic scheme for the main anodic process.

2. Experimental section

2.1. Chemicals

The p-dimethylaminobenzaldehyde (Aldrich, 98%) and the p-methoxyacetophenone (AcrosOrganic, 98%) were commercially purchased and used as received. The Nitromethane (Aldrich) was used in the electrochemical study. The tetraethylammonium tetrafluoroborate (TEAF) used in the preparative scale electrolysis, while, the tetrabutylammonium tetrafluoroborate (TBAF) used in the voltammetric study. The diethyl ether and the Ethanol were from Novachim. The Chloroform was from Scharlau.

2.2. Electrochemical techniques

The voltammetric study was performed with a Voltalab10 apparatus from Radiometer driven by the Volta Master software. All cyclic voltammetric measurements were conducted at room temperature in 25 mL of CH_3NO_2 solution containing TBAF (0.1 M) as a supporting electrolyte. The three-electrode system contained a platinum disk (2 mm diameter) as the working electrode, Ag/AgCl/KCl (saturated) as the reference electrode, and a platinum wire as the auxiliary electrode. The measurements were carried out with seven different potential scan rates (20–300 mVs^{-1}). The ohmic drop compensation was activated during all experiments. The measurements were performed at room temperature and the cell was briefly deoxygenated with azote before each scan.

The number of exchanged electrons (n_e) at the first oxidation peak of DMAMC was obtained from the comparison of the peak current to the mono-electronic oxidation peak of the ferrocenylchalcone (Fe-cha) recorded in the same conditions.

The preparative electrolysis was carried out in a two-compartment cell under a nitrogen atmosphere, at a constant potential of 1 V/ Ag/AgCl/KCl reference electrode. The separation between cell compartments was realized by a number 4 glass frit. A Voltalab10 apparatus from Radiometer guided by the Volta Master software was used. The anodic compartment contained one gram (1 g) of the DMAMC dissolved in 50 mL ($\approx 710^{-2}$ M) of a nitromethane solution containing tetraethylammonium tetrafluoroborate TEAF (0.1 M) as supporting electrolyte. The working electrode and the counter electrode were 2 cm x 2 cm platinum gauze. Homogenization of the solution was assured by a magnetic stirring. The electrolysis solutions were washed with water to eliminate

TEAF and to minimize the volume of nitromethane. The organic phase was dried with anhydrous Na_2SO_4 , concentrated and then precipitated in diethyl ether.

2.3. Material characterization

The ^1H NMR and ^{13}C NMR spectral data were acquired on a Bruker AV 300 spectrometer. FTIR analysis was performed with a Perkin Elmer Spectrum Two ATR-FTIR spectrometer, over the wave number range between 500 and 3500 cm^{-1} .

The UV-vis absorption spectra were seized on a Cary 5000 spectrophotometer. The PL spectra were carried out using laser diode emitting as an excitation source ($\lambda_{\text{ex}} = 375$ nm). The thermogravimetric analysis (TGA) was acquired on TA Instruments Q50 (TA Instruments, USA) at a heating rate of 10 $^\circ\text{C min}^{-1}$, under nitrogen.

For the gel permeation chromatography analysis, a μ styragel 500 A-15 mm column was used (with a length of 300 mm and a diameter of 7.8 mm). The temperature was 30 $^\circ\text{C}$. The solvent was tetrahydrofuran with a flow rate of 0.85 mL min^{-1} . Polystyrene was used as a standard.

2.4. Synthesis of 4-dimethylamino-4'-methoxychalcone (DMAMC)

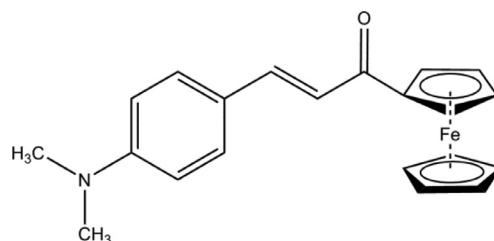
The general synthetic strategy employed to prepare the DMAMC (see Scheme 1) was based on Claisen-Schmidt condensation. The p-dimethylaminobenzaldehyde was treated with equimolar quantity of the p-methoxyacetophenone in a basic solution of sodium hydroxide (1.5 eq) in ethanol, at room temperature. The filtered product was purified by recrystallization from a water-ethanol mixture.

DMAMC: Yield 70%, yellow powder. ^1H NMR (ppm): 3.04 (s, 6H), 3.88 (s, 3H), 6.71 (d, 2H, $J = 8.7$ Hz), 6.94 (d, 2H, $J = 8.7$ Hz), 7.31 (d, 1H, $J = 15.6$ Hz), 7.53 (d, 2H, $J = 8.7$ Hz), 7.74 (d, 1H, $J = 15.6$ Hz), 7.99 (d, 2H, $J = 9$ Hz). ^{13}C NMR (ppm): 39–54.86–111.44–113.18–116.59–122.64–129.64–129.97–131.55–144.29–151.49–162.50–188.39. $M_p = 112$ $^\circ\text{C}$.

The ferrocenylchalcone Fe-cha (see Scheme 2), chosen as a reference in cyclic voltammetry, was prepared directly from acetylferrocene and p-(dimethylamino)benzaldehyde according to the previously described procedure [33,34].

Fe-cha: Yield 56%, red powder. ^1H NMR (ppm): 3.21 (s, 6H), 4.23 (s, 5H), 4.57 (s, 2H), 4.94 (s, 2H), 6.75 (d, 2H), 7.02 (d, 1H, $J = 9$ Hz), 7.72 (d, 2H), 7.81 (d, 2H, $J = 9$ Hz), 7.72 (d, 2H), 7.81 (d, 1H, $J = 9$ Hz). ^{13}C NMR (ppm): 40–69–70–72–81–112–117–122.5–130–142–152–193. $M_p = 140$ $^\circ\text{C}$.

The electrochemical properties of the Fe-cha were measured at a platinum working electrode in nitromethane 10^{-1} M TBAF solution. The cyclic voltammetry analyses showed a reversible one-electron oxidation at $E_{\text{pa}} = 0.673$ V versus Ag/AgCl when $\nu = 0.1$ Vs^{-1} (Fig. 1). The variation of the oxidation peak of Fe-cha with the scan rate was studied. The peak potential separation (ΔE_p) was close to 0.06 V and the anodic to cathodic current ratio was equal to unity, irrespective of changing sweep rate.



Scheme 2. The chemical structure of the ferrocenylchalcone (Fe-cha).

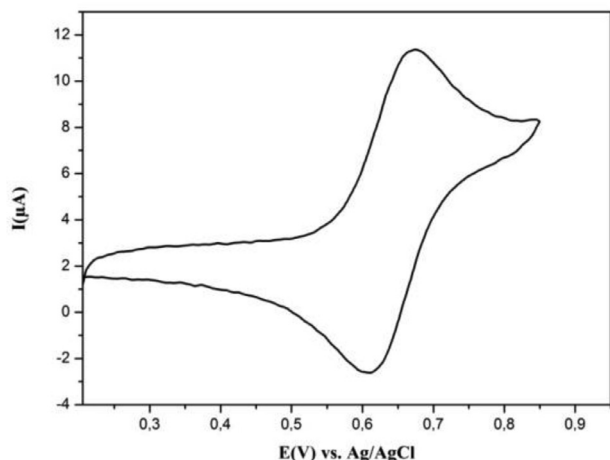


Fig. 1. Cyclic voltammogram corresponding to the oxidation of Fe-cha, 10^{-3} M in CH_3NO_2 , 10^{-1} M TBAF; recorded at a platinum electrode disk ($d=2$ mm), scan rate v : 100 mVs^{-1} , Counter electrode: Pt wire.

2.5. Method of calculations

All calculations for the oxidized TMC have been performed using the most popular Becke's three-parameter hybrid functional, B3 [35], with non-local correlation of Lee-Yang-Parr, LYP, abbreviated as B3LYP, method [36]. This method, based on Density Functional Theory (DFT) for a uniform electron gas (local spin density approximation), is used with the 6-31 g (d,p) basis set. An open-shell spin-unrestricted formalism was used for oxidized structure with unpaired electrons (UB3LYP). All calculations reported in this work were carried out with Gaussian 98 program [37].

3. Results and discussion

3.1. Voltammetric study

The cyclic voltammetry characterization of DMAMC in nitromethane ($0.1 \text{ M NBu}_4\text{BF}_4$) was carried out on a platinum disk for different concentrations and at different scan rates ranging from 20 to 300 mVs^{-1} . At 100 mVs^{-1} and for a substrate concentration $C = 2.10^{-3} \text{ M}$, the cyclic voltammogram exhibited two anodic peaks. The first is chemically irreversible at a potential close to 0.760 V , the second one is reversible and appears at 1.300 V / ECS, as shown in Fig. 2.

Moreover, taking no account of the difference between the diffusion coefficients D_{DMAMC} and $D_{\text{Fe-cha}}$, the number of electrons exchanged (n_e) at the first oxidation peak of DMAMC is close to one electron. This was obtained from the comparison of the peak current of DMAMC to the one of the monoelectronic ferrocene/ferrocenium redox system of the Fe-cha recorded in the same conditions [1,2]. It is worthy to note that the second peak current is approximately one half of the first. This result corroborates that the second peak corresponds to the reversible oxidation of a dimeric species.

To fully understand the mechanism of the electrochemical process, the variation of the peak potential of DMAMC with the scan rate or substrate concentration was studied. In anhydrous nitromethane, the first peak potential variation is a linear function of both the logarithms of the potential scan rate v and DMAMC concentration (C_i). The corresponding slopes are close to 20 mV (Fig. 3) and -20 mV per decade of v and (C_i/v), respectively (Fig. 4).

From this voltammetry study we conclude that the introduction of dimethylamine donor group raises the HOMO energy level

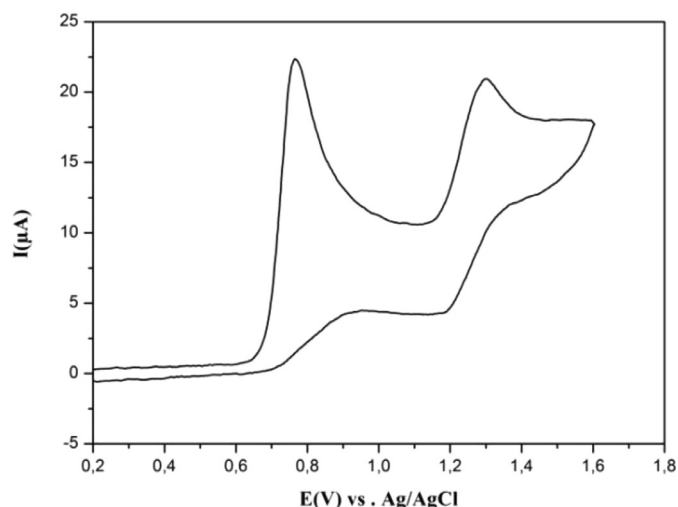


Fig. 2. Cyclic voltammogram for oxidation of DMAMC, 2.10^{-3} M in CH_3NO_2 ; Scan rate v : 100 mVs^{-1} .

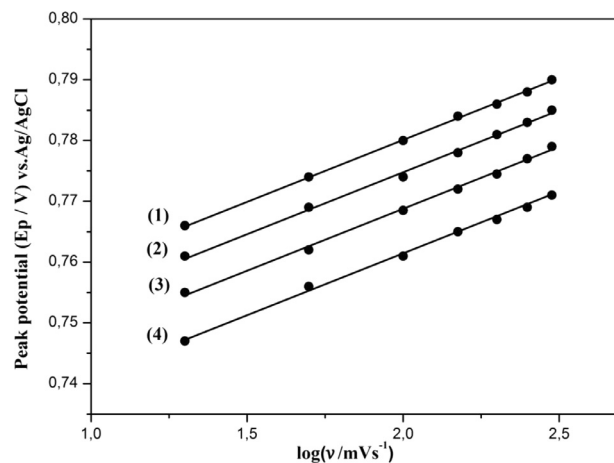


Fig. 3. Variation of the first peak potential E_p as a function of the logarithm of the scan rate v , for DMAMC in CH_3NO_2 , 10^{-1} M TBAF; (1) $C_1 = 0.5 \text{ mM}$, (2) $C_2 = 1 \text{ mM}$, (3) $C_3 = 2 \text{ mM}$, (4) $C_4 = 5 \text{ mM}$.

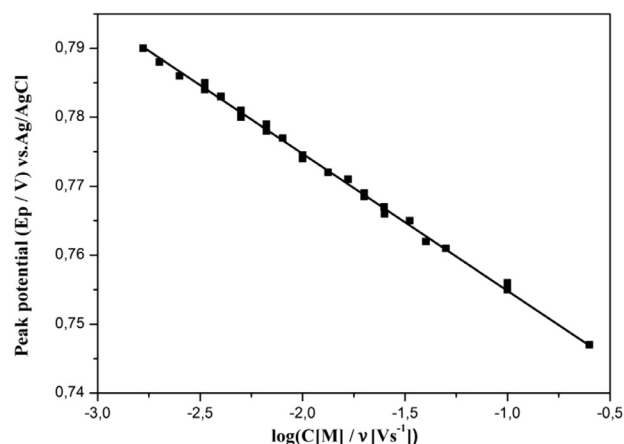


Fig. 4. Variation of the first peak potential E_p as a function of $\log(C_i/v)$ (C_i concentration in M, v scan rate in mVs^{-1}), for DMAMC in CH_3NO_2 , 10^{-1} M TBAF.

and greatly facilitates the anodic oxidation. In fact, the first peak potential of the studied chalcone was lowered by 0.83 V and 0.59 V compared to chalcones 4-methoxylated (MC) and 3,4,5-trimethoxylated (TMC) on ring B, respectively [1,2]. However, at the voltammetry timescale, the mechanism at the electrode, in a similar way to previous studies, remains governed by a rate deter-

Table 1
Positions and assignments of the IR vibration bands for DMAMC and O-DMAMC [27,38,39].

Mode assignment	Wavenumber (cm ⁻¹)	
	DMAMC	ODMAMC
C-H stretching	3005	3008
CH ₃ -O- / CH ₃ -N- protons stretching	2895/2803	2898/2808
C=O stretching	1600	1600
C=C stretching	1521	1508
C-N-C stretching	1305-1244	1360-1254
C-O-C stretching	1244-1160	1254-1167
C=C-H ethylenic out of plane bending (trans di substituted)	986	Absent
C=C-H ethylenic out of plane bending (trans tri substituted)	Absent	946
C=C-H aromatic out of plane bending	813	815-900
C=C ethylenic out of plane bending	561	Absent

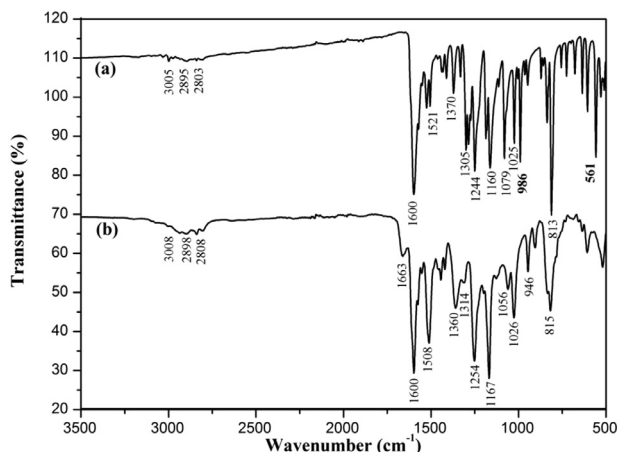


Fig. 5. IR spectra of DMAMC (a) and O-DMAMC (b).

mining second-order homogeneous reaction succeeding a fast first electron transfer. Most probably this reaction is a radical-radical coupling reaction.

3.2. Preparative scale electrolysis

In the light of the cyclic voltammetry results, preparative electrolysis of DMAMC were carried out in a separated cell at a constant potential as described in the experimental section. The electrolysis was stopped after consumption of 2 F/mole of the starting material. The solution obtained at the end of the electrolysis was handled as described in the experimental section. After precipitation in diethyl ether, a brown powder, corresponding to the expected oligomer, was collected by filtration. The rough yield, calculated from the ratio of the weight of collected powder by the weight of the starting material, was around 32%. The obtained powder is soluble in most organic solvents such as chloroform, dichloromethane and acetone.

3.3. Structure characterization of the electrolysis product

3.3.1. IR spectroscopy

The recorded FT-IR spectra for DMAMC and the collected powder are shown in Fig. 5. Both compounds present almost the same infrared spectral pattern. However, we note that the IR spectrum of the starting chalcone possesses needle-sharp bands whereas the powder's spectrum exhibits bands of broader width. These large bands are characteristic of oligomeric materials. In fact, the presence of a complex mixture of rotamers and chains with different lengths, in the oligomer powder, results in the band broadening. The GPC analysis confirmed the formation of a short-chain oligomer deriving from DMAMC (O-DMAMC) with an average degree of polymerization (DP) close to 3 and a dispersity of 1.2.

The most important bands and their attribution are depicted in Table 1.

We notice that the bands located at 561 and 986 cm⁻¹ disappeared in the oligomer spectrum. These bands are attributed of the C=C double bond of the ethylenic group in the enone linkage and the out of plane bending of H-C band (HC=CH, E configuration), respectively. However, new bands appeared at 900 and 946 cm⁻¹. These bands were assigned to the C=C-H aromatic out of plane bending of a 1,2,4 tri substituted benzene ring and the C=C-H ethylenic out of plane bending of a trans tri substituted alkene, respectively [39]. These results corroborate the involvement of both the vinyl group and the phenyl ring (B) of chalcone in the coupling reaction.

3.3.2. ¹H NMR and ¹³C NMR spectroscopy

The ¹H NMR spectrum of DMAMC (Fig. 6a) showed two signals at 3.04 and 3.88 ppm attributed to the dimethylamine and methoxy protons, respectively. The multiplet resonance signals at chemical shift 6.71–8.04 ppm were assigned to the aromatic protons. In this region, doublets of the ethylenic protons appeared at 7.74 ppm (*J* = 15.6 Hz) and 7.31 ppm (*J* = 15.6 Hz), showing that the ethylene moiety is in the trans-configuration E. The spectrum of the obtained powder (Fig. 6b) exhibited three broad resonance peaks, at the same shift as the DMAMC, attributed to the dimethylamine, methoxy and aromatic protons, respectively.

Finally, we noted that the integral ratio of the two signals (methyl amine protons/methoxy protons) is 1.9. This value is under the expected stoichiometric value 2.

The ¹³C NMR spectra of DMAMC and the oligomer O-DMAMC are shown in Figs. 7 and 8, respectively. Carbons of DMAMC are assigned as depicted by Fig. 6. In addition to signals appearing at almost the same chemical shifts as for the starting monomer, the oligomer spectrum showed the presence of new signals around 120 and 150 ppm. The ¹³C NMR spectrum recorded with DEPT using a 135° pulse (Fig. 7b) showed that the new signals corresponds to quaternary carbons. Moreover, this spectrum showed that the ethylenic carbon peaks of the chain ends are strongly attenuated (116–144 ppm). Finally, the signals relating to the carbons of the carbonyl group appear in the region ranging from 190 to 200 ppm indicating that these carbons have different surrounding chemical environments. These results confirmed that the coupling reaction occurred via an unsymmetrical linkage between the vinyl group and the phenyl ring (B) of the chalcone, leading to a phenylenevinylene like oligomer [1,2].

3.4. Optical study

The UV-visible absorption spectra of the DMAMC and the oligomer O-DMAMC in dilute chloroform solution are shown in Fig. 9. The UV-visible spectrum of the DMAMC revealed two bands with maxima located at 288 nm and 410 nm corresponding to n-π* (B II) and π-π* (B I) transitions, respectively.

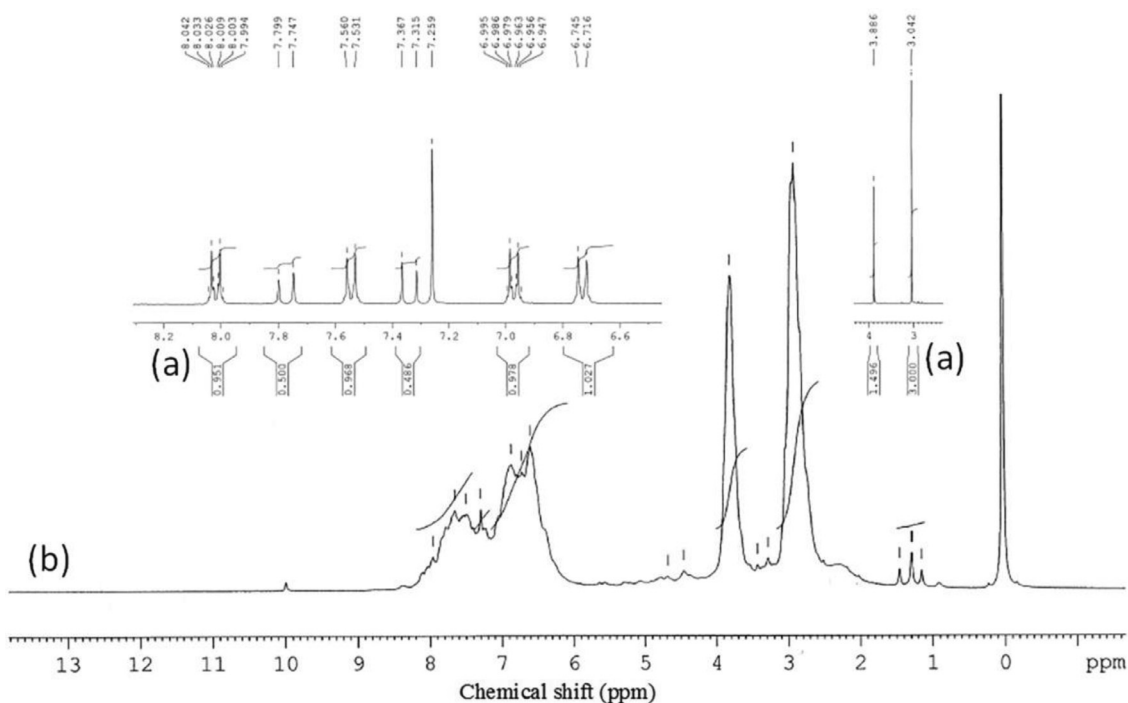


Fig. 6. ^1H NMR spectra of the DMAMC (a) and the O-DMAMC (b).

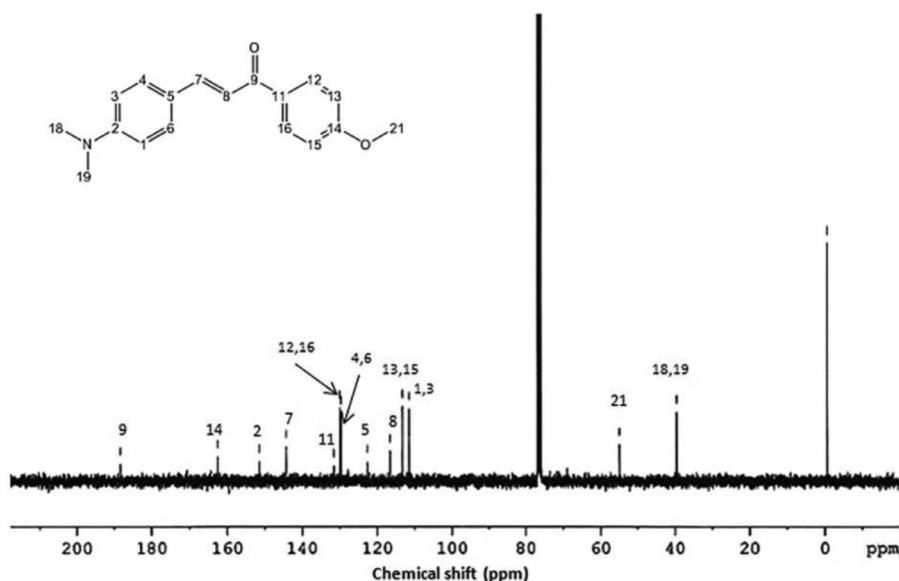


Fig. 7. ^{13}C NMR spectrum of DMAMC.

The first was attributed to the substituted benzoyl chromophore ($\text{ArCO}-$). The second band was attributed to the substituted cinnamoyl chromophore ($\text{ArCH}=\text{CH}-\text{CO}-$) implicating the whole conjugated system corresponding to the intramolecular charge transfer from the electron-donor amine substituent to the carbonyl group acting as an electron acceptor. The oligomer spectrum exhibited one absorption band located at 280 nm. Moreover, this spectrum presents two shoulders at around 410 and 524 nm, the first one of which is attributed to the $\text{ArCH}=\text{CH}-\text{CO}-$ conjugated system absorption in a similar way than the chalcone DMAMC.

The photoluminescent properties of the O-DMAMC were investigated in solution and as thin solid film (Fig. 10) under the UV light excitation ($\lambda_{\text{ex}} = 375$ nm). The recorded spectrum revealed two emission maxima at about 560 and 610 nm (Fig. 10).

A slight difference was observed for the emission spectrum of O-DMAMC in the thin film state indicating negligible interaction between solid states conjugated systems. Indeed, the presence of relatively large groups considerably limits the stacking of oligomers chains.

The optical study of the obtained material confirmed its semi-conducting character. The broad emission spectrum could be connected to the presence of oligomers with various conjugation lengths [40]. The optical gap, deduced from the absorption onset, was calculated to be 2.04 eV for the oligomer in solution.

The cyclic voltammetry (CV) studies of the O-DMAMC were investigated to determine the redox behavior and then to assess the HOMO and LUMO energy levels according to a reported empirical method [41–43]. The calculated E_{HOMO} , E_{LUMO} and $E_{\text{g-el}}$ values were found to be -4.99 eV, -3.31 eV and 1.68 eV, respectively.

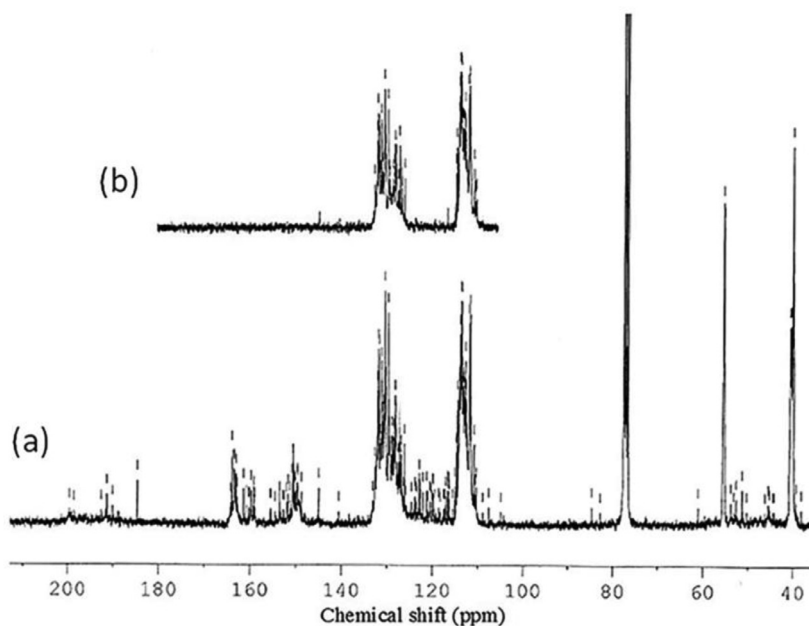


Fig. 8. ^{13}C NMR spectrum of the oligomer O-DMAMC.

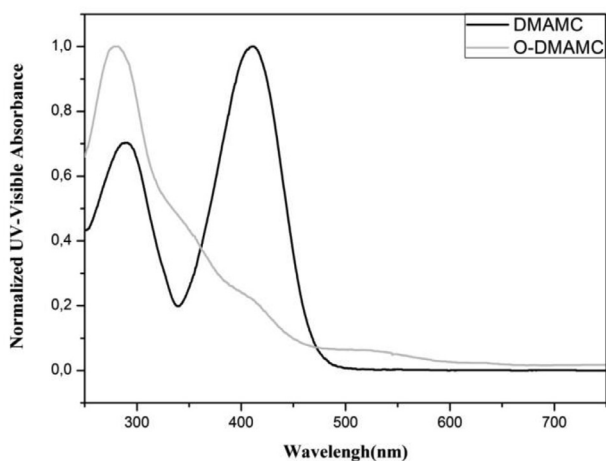


Fig. 9. UV-visible absorption spectra of DMAMC (black line) and the oligomer O-DMAMC (gray line), in chloroform solution.

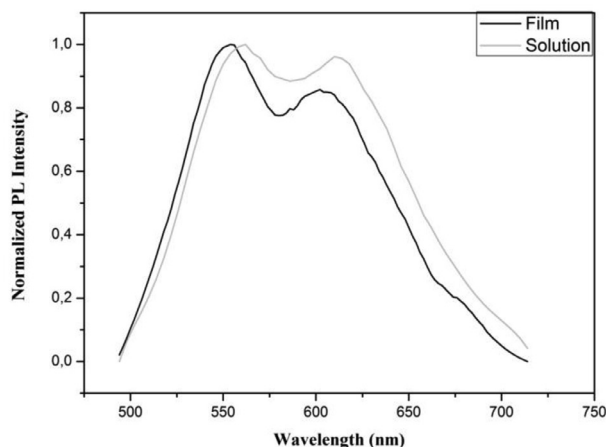


Fig. 10. Photoluminescence spectrum of O-DMAMC ($\lambda_{\text{ex}} = 375 \text{ nm}$).

Table 2

Electrochemical and optical gap and $\lambda_{\text{emission}}$ of oligomers deriving from methoxylated chalcone (O-MC) trimethoxylated Chalcone (O-TMC) and O-DMAMC.

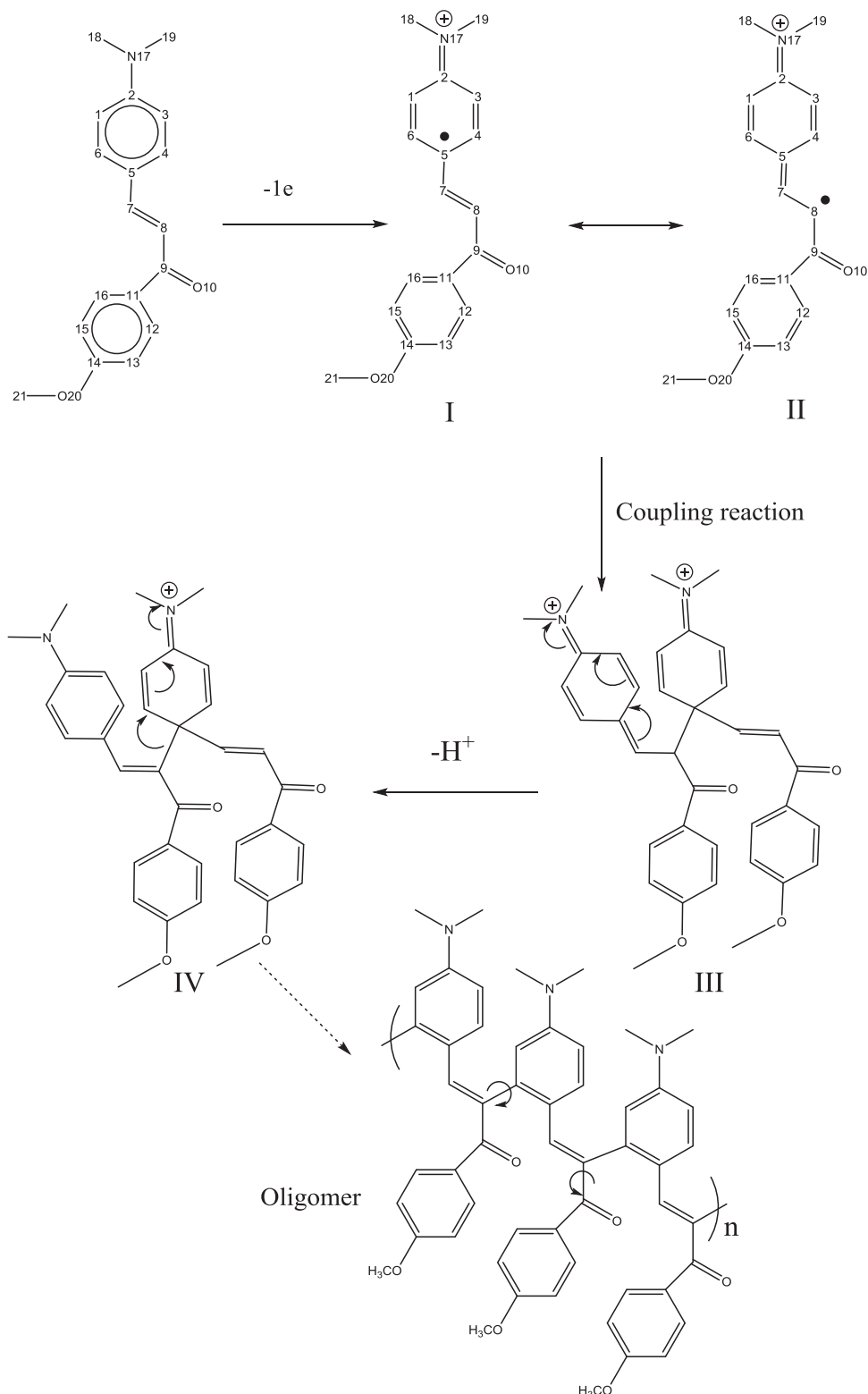
	Eg-el (eV)	Eg-op (eV)	$\lambda_{\text{emission}}$ (nm)
O-MC	2.86	3.15	390
O-TMC	2.99	3.09	445
O-DMAMC	1.68	2.04	560–610

To compare the optoelectronic properties of O-DMAMC to those of oligomers deriving from methoxylated chalcone (O-MC) trimethoxylated Chalcone (O-TMC), the corresponding electrochemical and optical gap, and the $\lambda_{\text{emission}}$ were summarized in Table 2.

The obtained values confirmed the strong dependence of these properties to the action of the dimethyl amine chromophore as a stronger donating group. This effect was traduced by a significant band-gap energy decrease and a light emission redshift. Notes that the observed difference between the bandgaps obtained from the optical method and from electrochemical analysis has been previously reported and explained for other conjugated polymers [44]. In fact, the optical electron transition leads to the formation of excited states, whereas the electrochemical reduction/oxidation generate species in ground states. Indeed, during the electrochemical reactions other thermodynamic (salvation...) and kinetic effects are involved and could affect the onset potential of the electrochemical reaction.

3.5. Thermal analysis

The thermal behavior of the oligomer was investigated by thermogravimetric analysis (TGA). In fact, the thermal behavior of the organic semi-conducting materials is an important property for both processing and applications [45]. The obtained thermogram is shown in Fig. 11. The continuous curve represents the loss of mass and the dotted line gives its derivative with respect to the temperature. TGA measurements revealed that the synthesized material has a thermal stability until 190 °C. Beyond this temperature, the obtained oligomer underwent a continuous multistep degradation most probably corresponding to the decomposition of the



Scheme 3. Electro-oligomerization mechanism.

pendant chains and the conjugated backbone, successively. Finally, the oligomer exhibited acceptable thermal stability for optoelectronic applications.

3.6. Electro-oligomerization mechanism

The obtained results showed that the oxidation of chalcone leads to the formation of a semi-conducting conjugated material.

The polymerization mechanism can be considered as sequences of coupling of radical cations and deprotonation reactions as previously proposed for the electro-oligomerization of methoxylated chalcones [1,2]. In fact, the voltammetric study indicated that the rate-limiting step is the coupling of two radical cations issued from the first electron transfer. This reaction involves two distonic isomers leading to a non-symmetric radical cations coupling. In fact, two mesomeric forms involving the donating effect of the amino

Table 3
The bond lengths for DMAMC and its radical cation (RC).

Bond (Å°)	C1-C2	C2-C3	C3-C4	C4-C5	C5-C6	C6-C1	C5-C7	C7-C8	C8-C9	C9-O ₁₀	C2-N ₁₇
DMAMC	1.415	1.418	1.384	1.409	1.407	1.387	1.457	1.352	1.478	1.232	1.381
RC	1.433	1.435	1.369	1.427	1.425	1.371	1.434	1.366	1.498	1.232	1.351

Table 4
The charge and the spin density distribution over DMAMC and its radical cation (RC).

	C1	C2	C3	C4	C5	C6	C7	C8	C9	N17	O10
DMAMC ^a	-0.134	0.354	-0.135	-0.128	0.128	-0.147	-0.107	-0.150	0.361	-0.508	-0.493
RC ^a	-0.099	0.366	-0.104	-0.104	0.146	-0.123	-0.100	-0.108	0.359	-0.465	-0.433
SD ^b	0.125	0.025	0.106	-0.048	0.246	-0.051	-0.085	0.304	-0.043	0.286	0.127

^a The Mulliken atomic charge (with hydrogen summed into heavy atom) for selected atoms.

^b The atomic spin density.

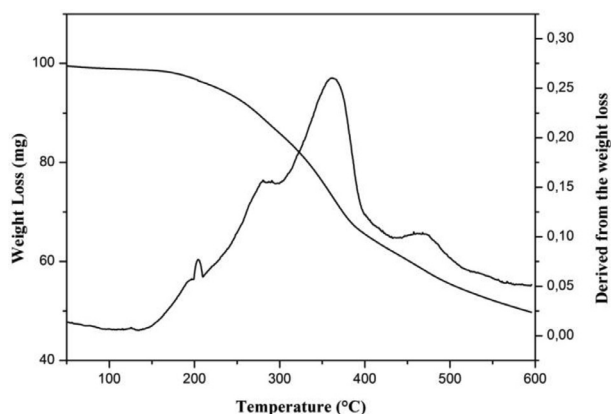


Fig. 11. TGA and DTG thermograms of the oligomer O-DMAMC.

group (I and II in Scheme 3) could describe the structure of the DMAMC radical cation.

This intuitive assumption was consolidated by the electronic structure of the DMAMC radical cation given by the DFT calculation. In Table 3 we present the bond lengths for DMAMC and its radical cation. The spin density distribution was given in Table 4. We note that the C-C bond lengths in the cinnamoyl moiety changed considerably in the radical cation structure. Specially, the C3-C4 and the C6-C1 bonds are close to localized double bond; however, the other bonds are longer than those of an aromatic ring. Moreover, the C2-N17 is shortened in the radical cation and a positive charge appeared on the nitrogen atom. Furthermore, Table 3 indicates that the highest SD was located on carbon C5 (0.246) and C8 (0.304).

All these results are in agreement with the isomeric forms previously described. Thus, it is most probably that the construction of a C-C linkage has been developed through the non-symmetric C5-C8 cross-coupling. This non-symmetric coupling seems presenting a good compromise between electronic and steric effects. The resulting hydrodimer (III) leads, after a proton loss, to the intermediate (IV). This latter cationic intermediate should be able to undergo an intramolecular rearrangement, under the aromatization driving force, leading to dimer with loss of a proton. This rearrangement occurs in a similar way than the acid catalysed rearrangement of 4,4' disubstituted cyclohexadienone [46–49]. The oxidation of the obtained dimer, leads to supplementary couplings with other oxidized monomers to form oligomers.

Unfortunately, it is not possible to describe rigorously the obtained oligomers structure because of the complexity of the pos-

sible stereostructures related to the trans-cis configuration. The presence of possible rotamers (s-cis / s-trans) relative to the conformation of the carbonyl groups further complicates this structural problem. Moreover, the calculated value of integral ratio of the methyl amine protons signal / methoxy protons signal, in 1HNMR study, may indicate that the oligomer suffer from a bond breaking side reaction resulting in the dimethylamine phenyl moiety loss. In fact, the carbon-carbon double bond cleavage of chalcones was previously described during their chemical oxidation. This oxidative cleavage mainly leads to the formation of the initial benzaldehyde and ketone. [50–54].

4. Conclusions

In this paper we have studied the anodic oxidation of a substituted chalcone, namely the 4-dimethylamino-4'-methoxychalcone (DMAMC), in nitromethane at a platinum working electrode. This work deals with the assessment of the dimethylamine group effect competing with methoxylated chalcone previously described. Regarding this objective we have showed that i) The presence of the dimethylamine group functional group keep unchanged the behavior of the studied chalcone at the voltammetry timescale and the mechanism at the electrode remains governed by a rate determining radical-radical coupling reaction. ii) The electro-oligomerization of chalcones remains the major reaction pathways at the preparative scale. Accordingly, a new o-phenylenevinylene oligomer was formed. The obtained oligomer was characterized by various spectroscopic techniques: ¹H and ¹³C NMR, FTIR and UV. The thermal study showed that the resulting material was stable up to 190 °C. The global electro-oligomerization mechanism reaction is similar to that proposed for methoxylated chalcone. The performed DFT calculation supported this mechanism and demonstrated that the dimethylamine group played a crucial role in conferring the distonic character to the radical cation, issued from the first electronic transfer, and consequently in directing the reaction scheme iii) The dimethylamine group notably influenced the absorption/emission properties of the obtained oligomer. In fact, the donating effect of the dimethylamine group resulted in a significant band-gap energy decrease and a light emission redshift.

Finally, in this contribution, we have brought out useful information for establishing correlation between the structural modifications of chalcones, their electrochemical reactivity and the absorption/emission properties of the resulting oligomer. In addition, we showed that the electro-oligomerization of chalcones is a promising facile synthetic route with a broad scope, a tolerance of functional groups and enable the access, with acceptable yields, to new organic semiconductors with modulated properties.

In the future, the optical and electrical properties of the obtained oligomer will be investigated for optoelectronic applications.

Declaration of Competing Interest

The authors declare that they have no known competing financial interests or personal relationships that could have appeared to influence the work reported in this paper.

CRediT authorship contribution statement

Ihlem Messaoudi: Investigation, Writing - original draft. **Imen Aribi:** Investigation. **Zouhour Zaaboub:** Investigation. **Sahbi Ayachi:** Investigation. **Mohamed Othman:** Investigation. **Ayoub Haj Said:** Conceptualization, Writing - original draft, Supervision.

Acknowledgements

This research was supported by the [Ministry of Higher Education and Scientific Research](#), Tunisia.

Supplementary materials

Supplementary material associated with this article can be found, in the online version, at doi:[10.1016/j.molstruc.2020.129810](https://doi.org/10.1016/j.molstruc.2020.129810).

References

- I. Aribi, S. Ghomrasni, S. Ayachi, K. Alimi, Sadok Roudesli, Ayoub Haj Said, Electro-synthesis, spectral and structural studies of a semi-conducting oligomer deriving from a methoxy-substituted chalcone, *J. Mol. Struct.* 1123 (2016) 276–283, doi:[10.1016/j.molstruc.2016.06.010](https://doi.org/10.1016/j.molstruc.2016.06.010).
- I. Aribi, S. Ayachi, K. Alimi, S. Roudesli, A. Haj Said, The anodic reactivity of 4,4'-dimethoxychalcone: a synthetic and mechanistic investigation, *Res. Chem. Intermed.* 43 (2017) 73–89, doi:[10.1007/s11164-016-2607-7](https://doi.org/10.1007/s11164-016-2607-7).
- S. Ghomrasni, I. Aribi, M. Chemek, A. Haj Said, K. Alimi, Some photophysical properties of new oligomer obtained from anodic oxidation of 4,4'-dimethoxychalcone, *Opt. Mater.* 78 (2018) 360–364, doi:[10.1016/j.optmat.2018.02.035](https://doi.org/10.1016/j.optmat.2018.02.035).
- P. Rajakumar, K. Visalakshi, S. Ganesan, P. Maruthamuthu, S.A. Suthanthiraraj, Pyreno-chalcone dendrimers as an additive in the redox couple of dye-sensitized solar cells, *J. Mater. Sci.* 47 (2012) 1811–1818, doi:[10.1007/s10853-011-5967-9](https://doi.org/10.1007/s10853-011-5967-9).
- E.D. D'silva, G.K. Podagatlapalli, S.V. Rao, S.M. Dharmaparakash, Study on third-order nonlinear optical properties of 4-methylsulfanyl chalcone derivatives using picosecond pulses, *J. Mater. Res. Bull.* 47 (2012) 3552–3557, doi:[10.1016/j.materresbull.2012.06.063](https://doi.org/10.1016/j.materresbull.2012.06.063).
- M.N. Arshad, A.M. Al-Dies, A.M. Asiri, M. Khalid, A.S. Birinji, K.A. Al-Amrya, A.A.C. Bragad, Synthesis, crystal structures, spectroscopic and nonlinear optical properties of chalcone derivatives: a combined experimental and theoretical study, *J. Mol. Struct.* 1141 (5) (2017) 142–156, doi:[10.1016/j.molstruc.2017.03.090](https://doi.org/10.1016/j.molstruc.2017.03.090).
- S. Shettigar, G. Umesh, K. Chandrasekharan, B.K. Sarojini, B. Narayana, Studies on third-order nonlinear optical properties of chalcone derivatives in polymer host, *J. Opt. Mater.* 30 (2008) 1297–1303, doi:[10.1016/j.optmat.2007.06.008](https://doi.org/10.1016/j.optmat.2007.06.008).
- L.M.G. Abegão, R.D. Fonseca, F.A. Santos, G.B. Souza, A.L.B.S. Barreiros, M.L. Barreiros, M.A.R.C. Alencar, C.R. Mendonça, D.L. Silva, L. De Boni, J.J. Rodrigues Jr., Second- and third-order nonlinear optical properties of unsubstituted and mono-substituted chalcones, *Chem. Phys. Lett.* 648 (2016) 91–96, doi:[10.1016/j.cplett.2016.02.009](https://doi.org/10.1016/j.cplett.2016.02.009).
- S.R. Maidur, P.S. Patil, S.V. Rao, M. Shkir, S.M. Dharmaparakash, Experimental and computational studies on second- and third-order nonlinear optical properties of a novel D- π -A type chalcone derivative: 3-(4-methoxyphenyl)-1-(4-nitrophenyl) prop-2-en-1-one, *Opt. Laser. Technol.* 97 (2017) 219–228, doi:[10.1016/j.optlastec.2017.07.003](https://doi.org/10.1016/j.optlastec.2017.07.003).
- P.S. Patil, S.R. Maidur, J.R. Jahagirdar, T.S. Chia, C.K. Quah, M. Shkir, Crystal structure, spectroscopic analyses, linear and third-order nonlinear optical properties of anthracene-based chalcone derivative for visible laser protection, *Appl. Phys. B* 125 (2019) 163, doi:[10.1007/s00340-019-7275-z](https://doi.org/10.1007/s00340-019-7275-z).
- S. Raghavendra, C.S. Chidan Kumar, T. Chandra Shekhara Shetty, B.N. Lakshminarayana, C.K. Quah, S. Chandraru, G.S. Ananthnag, R.A. Gonsalves, S.M. Dharmaparakash, Structure property relationship of a new nonlinear optical organic crystal: 1-(3,4-Dimethoxyphenyl)-3-(3-fluorophenyl)prop-2-en-1-one for optical power limiting applications, *Results Phys.* 7 (2017) 2550–2556, doi:[10.1016/j.rinp.2017.07.037](https://doi.org/10.1016/j.rinp.2017.07.037).
- B. Delavaux-Nicot, J. Maynadié, D. Lavabre, S. Fery-Forgues, Ca²⁺ vs. Ba²⁺ electrochemical detection by two disubstituted ferrocenyl chalcone chemosensors. Study of the ligand–metal interactions in CH₃CN, *J. Organomet. Chem.* 692 (2007) 874–886, doi:[10.1016/j.jorganchem.2006.10.045](https://doi.org/10.1016/j.jorganchem.2006.10.045).
- J. Prabhu, K. Velmurugan, A. Raman, N. Durairandy, M.S. Kiran, S. Easwaramoorthi, R. Nandhakumar, A simple chalcone based ratio-metric chemosensor for sensitive and selective detection of Nickel ion and its imaging in live cells, *J. Sens. Actuators B* 238 (2017) 306–317, doi:[10.1016/j.snb.2016.07.018](https://doi.org/10.1016/j.snb.2016.07.018).
- Y. Shan, Q. Wu, N. Sun, Y. Sun, D. Cao, Z. Liu, R. Guan, Y. Xu, X. Yu, Two indole chalcone derivatives as chemosensor for cyanide anions, *Mater. Chem. Phys.* 186 (2017) 295–300, doi:[10.1016/j.matchemphys.2016.10.056](https://doi.org/10.1016/j.matchemphys.2016.10.056).
- Y. Wei, G. Qin, W. Wang, W. Bian, S. Shuang, C. Dong, Development of fluorescent FeIII sensor based on chalcone, *J. Lumin.* 131 (2011) 1672–1676, doi:[10.1016/j.jlumin.2011.03.062](https://doi.org/10.1016/j.jlumin.2011.03.062).
- B. Delavaux-Nicot, J. Maynadié, D. Lavabre, S. Fery-Forgues, J. Organomet. Chem. 692 (2007) 3351–3362 Two electroactive ferrocenyl chalcones as original optical chemosensors for Ca²⁺ and Ba²⁺ cations in CH₃CN, doi:[10.1016/j.jorganchem.2007.03.044](https://doi.org/10.1016/j.jorganchem.2007.03.044).
- J. Maynadié, B. Delavaux-Nicot, D. Lavabre, S. Fery-Forgues, Monosubstituted ferrocenyl chalcones: effect of structural changes upon the ability to detect calcium by absorption spectroscopy, *J. Organomet. Chem.* 691 (2006) (2006) 1101–1109, doi:[10.1016/j.jorganchem.2005.11.021](https://doi.org/10.1016/j.jorganchem.2005.11.021).
- Z. Xu, W. Yang, C. Dong, Determination of human serum albumin using an intramolecular charge transfer fluorescence probe: 4'-dimethylamino-2,5-dihydroxychalcone, *Bioorg. Med. Chem. Lett.* 15 (2005) 4091–4096, doi:[10.1016/j.bmcl.2005.06.014](https://doi.org/10.1016/j.bmcl.2005.06.014).
- S.R. Annapoorna, M.P. Rao, B. Sethuram, Multiple substituent effects in the C=C reduction of phenyl styryl ketones: cyclic voltammetry as a tool, *J. Electroanal. Chem.* 490 (2000) 93–97, doi:[10.1016/s0022-0728\(00\)00166-2](https://doi.org/10.1016/s0022-0728(00)00166-2).
- L.D. Hicks, A.J. Fry, V.C. Kurzweil, Ab initio computation of electron affinities of substituted benzalacetophenones (chalcones): a new approach to substituent effects in organic electrochemistry, *Electrochim. Acta.* 50 (2004) 1039–1047, doi:[10.1016/j.electacta.2004.08.003](https://doi.org/10.1016/j.electacta.2004.08.003).
- J.Y. Alston, A.J. Fry, Substituent effects on the reduction potentials of benzalacetophenones (chalcones): improved substituent constants for such correlations, *Electrochim. Acta.* 49 (2004) 455–459, doi:[10.1016/j.electacta.2003.08.028](https://doi.org/10.1016/j.electacta.2003.08.028).
- P. Tompe, G. Clementis, I. Petnehazy, Z.M. Jaszay, L. Toke, Quantitative structure-electrochemistry relationships of α , β -unsaturated ketones, *Anal. Chim. Acta.* 305 (1995) 295–303, doi:[10.1016/0003-2670\(94\)00354-o](https://doi.org/10.1016/0003-2670(94)00354-o).
- Z. Saničanin, I. Tabaković, Electrochemical transformations of 2'-hydroxychalcones into flavonoids, *Tetrahedron Lett* 27 (1986) 407–408, doi:[10.1016/s0040-4039\(00\)84031-9](https://doi.org/10.1016/s0040-4039(00)84031-9).
- Z. Saničanin, I. Tabaković, Electrochemical synthesis of heterocyclic compounds—XVIII. Anodic oxidation of 2'-hydroxychalcones, *Electrochim Acta* 33 (1988) 1595–1600, doi:[10.1016/0013-4686\(88\)80230-5](https://doi.org/10.1016/0013-4686(88)80230-5).
- N. Cotellet, P. Hapiot, J. Pinson, C. Rolando, H. Vezin, Polyphenols Deriving from chalcones: investigations of redox activities, *J. Phys. Chem. B.* 109 (2005) 23720–23729, doi:[10.1021/jp0550661](https://doi.org/10.1021/jp0550661).
- K.M. Naik, S.T. Nandibewoor, Electrochemical behavior of chalcone at a glassy carbon electrode and its analytical applications, *Am. J. Anal. Chem.* 3 (2012) 656–663, doi:[10.4236/ajac.2012.39086](https://doi.org/10.4236/ajac.2012.39086).
- K.G. Komarova, S.N. Sakipov, V.G. Plotnikov, M.V. Alifimov, Luminescent properties of chalcone and its amino derivatives, *J. Lumin.* 164 (2015) 57–63, doi:[10.1016/j.jlumin.2015.03.021](https://doi.org/10.1016/j.jlumin.2015.03.021).
- K.H. Ibaouf, A.O. Elzupir, M.S. AlSalhi, A.S. Alaamer, Influence of functional groups on the photophysical properties of dimethylamino chalcones as laser dyes, *J. Optic. Mater.* 76 (2018) 216–221, doi:[10.1016/j.optmat.2017.12.034](https://doi.org/10.1016/j.optmat.2017.12.034).
- M. Gaber, S.A. El-Daly, T.A. Fayed, Y.S. El-Sayed, Photophysical properties, laser activity and photoreactivity of a heteroaryl chalcone A model of solvatochromic fluorophore, *Opt. Laser. Technol.* 40 (2008) 528–537, doi:[10.1016/j.optlastec.2007.08.006](https://doi.org/10.1016/j.optlastec.2007.08.006).
- M. Jadhav, J.V. Vaghasiya, D. Patil, S.S. Soni, N. Sekar, Effect of donor modification on the photo-physical and photo-voltaic properties of N-alkyl/aryl amine based chromophores, *New. J. Chem.* 43 (2019) 8970, doi:[10.1039/c8nj06196c](https://doi.org/10.1039/c8nj06196c).
- M. Jadhav, J. Vaghasiya, D. Patil, S. Soni, N. Sekar, Structure-efficiency relationship of newly synthesized 4-substituted donor- π -acceptor coumarins for dye-sensitized solar cells, *New J. Chem.* 42 (2018) 5267–5275, doi:[10.1039/c7nj04954d](https://doi.org/10.1039/c7nj04954d).
- D.G. Slobodinyuk, E.V. Shklyaeva, G.G. Abashev, Electrochemical oxidation of asymmetric chalcones containing two terminal electroactive moieties, *J. Appl. Electrochem.* 50 (2020) 757–766, doi:[10.1007/s10800-020-01434-z](https://doi.org/10.1007/s10800-020-01434-z).
- Y. Jung, K.I. Son, Y.E. Oh, D.Y. Noh, Ferrocenyl chalcones containing anthracenyl group: synthesis, X-ray crystal structures and electrochemical properties, *J. Polym. Sci.* 27 (2008) 861–867, doi:[10.1016/j.poly.2007.11.015](https://doi.org/10.1016/j.poly.2007.11.015).
- J. Maynadié, B. Delavaux-Nicot, D. Lavabre, B. Donnadié, J.-C. Daran, A. Sournia-Saquet, From Calcium Interaction to Calcium Electrochemical Detection by [(C₅H₅)Fe(C₅H₄COCH=CHC₆H₄NET₂)] and Its Two Novel Structurally Characterized Derivatives, *Inorg. Chem.* 43 (6) (2004) 2064–2077, doi:[10.1021/ic0345828](https://doi.org/10.1021/ic0345828).
- A.D. Becke, Density-functional thermochemistry. III. The role of exact exchange, *J. Chem. Phys.* 98 (1993) 5648–5652, doi:[10.1063/1.464913](https://doi.org/10.1063/1.464913).
- C. Lee, W. Yang, R.G. Parr, Development of the Colle-Salvetti correlation-energy formula into a functional of the electron density, *Phys. Rev. B* 37 (1988) 785–789 W.J. Pietro, M.M. Francl, W.J. Hehre, D.J. Defrees, J.A. Pople, J.S. Binkley, Self-consistent molecular orbital methods. 24. Supplemented small split-valence basis sets for second-row elements, *J. Am. Chem. Soc.* 104 (1982) 5039–5048. doi:[10.1021/ja00383a007](https://doi.org/10.1021/ja00383a007), doi:[10.1103/PhysRevB.37.785](https://doi.org/10.1103/PhysRevB.37.785).

- [37] M.J. Frisch, G.W. Trucks, H.B. Schlegel, G.E. Scuseria, M.A. Robb, J.R. Cheeseman, V.G. Zakrzewski, J.A. Montgomery Jr., R.E. Stratmann, J.C. Burant, S. Dapprich, J.M. Millam, A.D. Daniels, K.N. Kudin, M.C. Strain, O. Farkas, J. Tomasi, V. Barone, M. Cossi, R. Cammi, B. Mennucci, C. Pomelli, C. Adamo, S. Clifford, J. Ochterski, G.A. Petersson, P.Y. Ayala, Q. Cui, K. Morokuma, D.K. Malick, A.D. Rabuck, K. Raghavachari, J.B. Foresman, J. Cioslowski, J.V. Ortiz, B.B. Stefanov, G. Liu, A. Liashenko, P. Piskorz, I. Komaromi, R. Gomperts, R.L. Martin, D.J. Fox, T. Keith, M.A. Al-Laham, C.Y. Peng, A. Nanayakkara, C. Gonzalez, M. Challacombe, P.M.W. Gill, B. Johnson, W. Chen, M.W. Wong, J.L. Andres, C. Gonzalez, M. Head-Gordon, E.S. Replogle, J.A. Pople, Gaussian 98, Revision A.6, Gaussian, Inc., Pittsburgh PA, 1998.
- [38] G. Vanangamudi, M. Subramanian, P. Jayanthi, R. Arulkumar, D. Kamalakkannan, G. Thirunarayanan, IR and NMR spectral studies of some 2-hydroxy-1-naphthyl chalcones: assessment of substituent effects, Arab. J. Chem. 9 (2016) S717–S724, doi:10.1016/j.arabjc.2011.07.019.
- [39] M.D. Mayo, F.A. Miller, W.H. Robert, Course Notes on the Interpretation of Infrared and Raman Spectra, John Wiley, Hoboken, New Jersey, 2004 first ed..
- [40] T.E. Schuler, S.H. Wang, P. Shirley, R.K. Onmori, Synthesis and characterization of semiconductor polymers having different phenylene–vinylene conjugation lengths, J. Mater. Sci. 43 (2008) 541–545, doi:10.1007/s10853-007-1710-y.
- [41] J.L. Bredas, R. Silbey, D.S. Boudreau, R.R. Chance, Chain-length dependence of electronic and electrochemical properties of conjugated systems: polyacetylene, polyphenylene, polythiophene, and polypyrrole, J. Am. Chem. Soc. 105 (1983) 6555, doi:10.1021/ja00360a004.
- [42] J. Pommerehne, H. Vestweber, W. Guss, R.F. Mahrt, H. Bassler, M. Porsch, J.J. Daub, Efficient two layer leds on a polymer blend basis, Adv. Mater. 7 (1995) 551, doi:10.1002/adma.19950070608.
- [43] Y. Zhu, A.R. Rabindranath, T. Beyerlein, B. Tieke, Highly Luminescent 1,4-Diketo-3,6-diphenylpyrrolo[3,4-c]pyrrole- (DPP-) based conjugated polymers prepared upon suzuki coupling, Macromolecules 40 (2007) 6981, doi:10.1021/ma0710941.
- [44] S.B. Amor, A.H. Said, M. Chemek, F. Massuyeau, J. Wéry, E. Faulques, K. Alimi, S. Roudesli, Synthesis and optical study of a new oligophenylene polymers, 4 (2012) 1226–124. 10.3390/polym4021226
- [45] H. Wang, X. Tao, E. Newton, Thermal degradation kinetics and lifetime prediction of a luminescent conducting polymer, J. Polym. Int. 53 (2004) 20–26, doi:10.1002/pi.1279.
- [46] J.N. Marx, Y.-S.P. Hahn, Acid-catalyzed migration of the vinyl substituent in the dienone–phenol rearrangement, J. Org. Chem. 53 (1988) 2866–2868, doi:10.1021/jo00247a046.
- [47] B. Miller, The Mechanism of 1,3-Migrations of Allyl Groups in the Dienone–Phenol Rearrangements of 2,6-Di-*t*-butylcyclohexadienones, J. Am. Chem. Soc. 87 (1965) 5111–5115, doi:10.1021/ja00950a023.
- [48] J.N. Marx, J.C. Argyle, L.R. Norman, Migration of electronegative substituents. I. Relative migratory aptitude and migration tendency of the carboxy group in the dienone–phenol rearrangement, J. Am. Chem. Soc. 96 (1974) 2121–2129, doi:10.1021/ja00814a022.
- [49] A.H. Said, F. Matoussi, C. Amatore, J.-N. Verpeaux, Mechanistic investigation of the anodic oxidation of *p*-methoxytoluene in dry and wet acetonitrile, J. Electroanal. Chem. 464 (1999) 85–92, doi:10.1016/s0022-0728(98)00477-x.
- [50] K. Kurosawa, J. Higuchi, Bull study on oxidation of chalcones with lead tetraacetate and manganic acetate, Chem. Soc. Jpn. 45 (1972) 1132–1136, doi:10.1246/bcsj.45.1132.
- [51] S.R. Annapoorna, M.P. Rao, B. Sethuram, Study of interactive free-energy relationships on ruthenium(III) catalyzed oxidation of phenyl styryl ketone and its substituted analogues by V(V) in acid medium, Int. J. Chem. Kinet. 32 (2000) 581–588, doi:10.1002/1097-4601(2000)32:10<581::AID-KIN1>3.0.CO;2-K.
- [52] A. Dhakshinamoorthy, K. Pitchumani, Clay-supported ceric ammonium nitrate as an effective, viable catalyst in the oxidation of olefins, chalcones and sulfides by molecular oxygen, Catal. Commun. 10 (2009) 872–878, doi:10.1016/j.catcom.2008.12.025.
- [53] A. Dhakshinamoorthy, K. Pitchumani, Clay-anchored non-heme iron–salen complex catalyzed cleavage of C=C bond in aqueous medium, Tetrahedron 62 (2006) 9911–9918, doi:10.1016/j.tet.2006.08.011.
- [54] V. Srinivasulu, M. Adinarayana, B. Sethuram, T.N. Rao, Kinetics and mechanism of OsO₄ catalyzed oxidation of chalcones by Ce⁴ in aqueous acetic sulfuric acid media, React. Kinet. Catal. Lett. 27 (1985) 167–172, doi:10.1007/bf02064480.